

Novel Iron(II) Microporous Spin-Crossover Coordination Polymers with Enhanced Pore Size

Francisco J. Muñoz-Lara,[†] Ana B. Gaspar,[†] M. Carmen Muñoz,[‡] Vadim Ksenofontov,[§] and José Antonio Real^{*,†}

[†]Institut de Ciència Molecular (ICMol)/Departament de Química Inorgànica, Universitat de València, C/ Catedrático José Beltrán Martínez 2, 46980 Paterna, València, Spain

[‡]Departamento de Física Aplicada, Universitat Politècnica de València, Camino de Vera s/n, 46022 València, Spain

[§]Institut für Anorganische und Analytische Chemie, Johannes-Gutenberg-Universität, Staudinger-Weg 9, D-55099 Mainz, Germany

Supporting Information

ABSTRACT: In this Communication, we report the synthesis and characterization of novel Hofmann-like spin-crossover porous coordination polymers of composition $\{\text{Fe}(\text{L})[\text{M}(\text{CN})_4]\}_n \cdot \text{G}$ [L = 1,4-bis(4-pyridylethynyl)benzene and $\text{M}^{\text{II}} = \text{Ni}, \text{Pd}, \text{and Pt}$]. The spin-crossover properties of the framework are closely related to the number and nature of the guest molecules included in the pores.

Porous coordination polymers¹ (PCPs), where the framework exhibits solid-state properties like magnetism,² luminescence,³ conductivity,⁴ or charge transport,⁵ which change concomitantly with the sorption/desorption of guest molecules, represent a new class of multifunctional materials. This new generation of PCPs acts by expressing the host–guest interactions in a sensory way.

Among PCP porous and magnetic properties, those porous polymers made up of bistable iron(II) building blocks are noteworthy. Iron(II) spin-crossover (SCO) building blocks present labile electronic configurations switchable between the high-spin (HS) and low-spin (LS) states in response to external stimuli (temperature, pressure, light, or absorption/desorption of an analyte). In the HS and LS states, the iron(II) SCO centers reveal differences in magnetism, optical properties, dielectric constant, color, and structure.⁶ For cooperative spin transitions (STs), this switch can be performed within the hysteresis loop based on the first-order hysteretic ST, which confers to the material a memory function.⁷ Thus, guest inclusion in the SCO framework can provoke stabilization of the Fe^{II} ions in the HS or LS state or has no effect. The resulting effect relies on the chemical nature and size of the guest molecules that occupy the pores. Detection of the sorption/desorption of guest molecules in the framework is performed by analysis of the magnetic and optical outputs (the temperature dependence of the magnetic susceptibility and/or by the change of color at a given temperature). In principle, a fingerprint in the form of a magnetic response pattern may be attainable for distinct analytes.

Examples of iron(II) SCO-PCPs reported up to now are still scarce. The first report on a microporous iron(II) polymer was based on the ligand 1,2-di(4-pyridyl)ethylene (dpe; trans

isomer)⁸ and dates back to 1995. Almost a decade later was published a detailed investigation of the guest influence on the SCO properties in analogous frameworks with composition $[\text{Fe}(\text{L})(\text{NCS})_2]_n \cdot \text{G}$ [L = 4,4'-azopyridine (azpy) and DL-1,2-bis(4'-pyridyl)-1,2-ethanediol (bped)].⁹ In these SCO-PCPs, the adsorption of guest molecules induces some stabilization of the framework in the LS state. Typically, they show a gradual SCO in the temperature region 10–200 K.

More recently, a drastic influence of the guest inclusion on T_c and cooperativity has been reported for the three-dimensional Hofmann-like SCO-PCPs $\{\text{Fe}(\text{L})[\text{M}(\text{CN})_4]\}_n \cdot \text{G}$ [L = pyrazine (pz);^{10–12} azpy,¹³ 4,4'-bis(pyridyl)acetylene (bpac),¹⁴ and dpe (trans isomer)¹⁵ and $\text{M}^{\text{II}} = \text{Ni}, \text{Pd}, \text{and Pt}$]. These types of frameworks provide two guest interactive sites, one between the organic bridges (site A) and another between the four-coordinate M centers (site B). Particularly interesting are the results obtained with the SCO-PCP $\{\text{Fe}(\text{pz})[\text{M}(\text{CN})_4]\}_n$. In fact, it represents a new generation of functional materials responding to their environment because the framework can allow reversible control of the magnetic and optical outputs through the chemical response at room temperature.^{10,11}

Further development of these polymers points at increasing the pore size and inner pore functionality. In this Communication, we report the synthesis and characterization of a novel family of iron(II) Hoffman-like three-dimensional coordination polymers $\{\text{Fe}(\text{bpeben})[\text{M}(\text{CN})_4]\}_n \cdot n\text{H}_2\text{O} \cdot 0.5\text{bpeben}$ [M = Pt, $n = 1.5\text{H}_2\text{O}$ (1) and $n = 0$ (2); M = Pd, $n = 1.5\text{H}_2\text{O}$ (3) and $n = 0$ (4); M = Ni, $n = 2$ (5) and $n = 0$ (6)], based on the organic pillar ligand 1,4-bis(4-pyridylethynyl)benzene (bpeben).¹⁶ These novel iron(II) coordination polymers exhibit SCO and enhanced porous properties.

The coordination polymers precipitate instantaneously as yellow-orange microcrystalline powders when a water solution of $\text{K}_2\text{M}(\text{CN})_4 \cdot n\text{H}_2\text{O}$ is added to a continuously stirring methanolic solution containing $\text{Fe}(\text{BF}_4)_2 \cdot 6\text{H}_2\text{O}$ and the ligand bpeben in equimolar amounts. Because of the great insolubility of these compounds, we were able to get single crystals only for 1. For the same reason, the quality of these crystals only enabled us to complete the crystallographic analysis at 120 K.

Received: July 26, 2012

Published: December 21, 2012

As for the analogous polymers with pz, dpe, azpy, and bpac pillar ligands, the crystal structure of **1** was solved in the $P4/mmm$ space group.^{10–15} STable1 in the Supporting Information (SI) gathers the relevant crystallographic data as well as bond lengths and angles. The structure is constituted of alternate octahedral $[\text{Fe}^{\text{II}}\text{N}_6]$ cationic centers and square-planar $[\text{Pt}(\text{CN})_4]^{2-}$ anions (Figure 1). The equatorial positions are

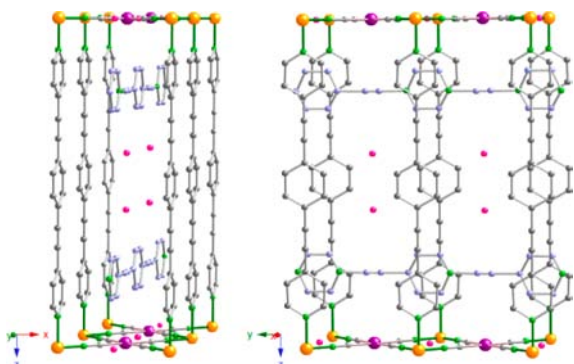


Figure 1. View of the crystal structure of **1** along the $[010]$ direction. Color code: N, green; C, gray and blue; Fe, orange; Pt, violet; $\text{O}(\text{H}_2\text{O})$, blue.

occupied by four N atoms of four equivalent $[\text{Pt}(\text{CN})_4]^{2-}$ groups, which act as bridges linking four Fe^{II} atoms, generating two-dimensional $\{\text{Fe}[\text{Pt}(\text{CN})_4]_{\infty}\}$ layers. The layers are pillared by the ligand bpeben along the $[001]$ direction, which occupies the axial positions of the Fe^{II} ions, thereby generating an open three-dimensional framework. The axial and equatorial Fe–N bond distances are consistent with Fe^{II} in the LS state, with Fe–N(1) = 1.99(2) Å and Fe–N(2) = 1.918(16) Å. The pores running parallel to the $[010]$ and $[100]$ directions are defined by the Fe–Fe distances through the pillar ligand bpeben and the anionic linkers $[\text{Pt}(\text{CN})_4]^{2-}$ with a gate size in the LS state of $20.49(3) \text{ \AA} \times 7.14(3) \text{ \AA}$. Inside the pores, there are half of a bpeben molecule and 1.5 H_2O molecules per Fe^{II} atom. Several host–guest weak intermolecular contacts between pillar and clathrated bpeben ligands are present $[\text{C}\cdots\text{N} [3.60(2)–3.865(9) \text{ \AA}]$ and $\text{C}\cdots\text{C} [3.64(2)–3.796(8) \text{ \AA}]$ (STable2 in the SI). The solvent is heavily disordered and has been modeled as such. There is also disorder observed in the clathrated bpeben ligand. However, while these issues reduce the quality of the structural model, none of them affect the conclusions drawn as to the atomic connectivity or network topology. The accessible volume of the framework without considering the guest molecules was determined to be 511 \AA^3 (198.9 \AA^3 considering the bpeben and H_2O guest molecules), which corresponds to 48.9% of the unit cell at 120 K [$1044.7(2) \text{ \AA}^3$] and is 2 times the order of magnitudes found for azpy, dpe, and bpac homologues.^{10–15}

Powder X-ray diffraction (PXRD) patterns for **2–6** were recorded at 293 K (see the SI). Compounds **2–6** have very similar profiles, with most of the significant peaks located at $2\theta = 4.2^\circ, 8.5^\circ, 12.75^\circ, 17.20^\circ, 18.04^\circ, 19.50^\circ, 21.5^\circ,$ and 24.9° . In particular, the peak at 4.2° corresponds to the separation between $\{\text{Fe}[\text{Pt}(\text{CN})_4]_{\infty}\}$ sheets. From these PXRD profiles and taking into account the analytical data [IR, energy-dispersive X-ray microanalysis, and CHN analysis] of compounds **2–6**, it is reasonable to propose that they are isostructural to **1**.

The water contents of **1**, **3**, and **5** have been established by thermogravimetric analyses (TGA). The compounds show similar TGA profiles. A smooth release of H_2O molecules occurs between room temperature and 400 K, followed by the decomposition process of the $\{\text{Fe}(\text{bpeben})[\text{M}(\text{CN})_4]\}$ framework and the bpeben guest molecule, which takes place as a multiple-step process in the interval 500–800 K.

The thermal dependences of $\chi_{\text{M}}T$ for **1–6** (χ_{M} stands for the molar magnetic susceptibility and T for the temperature) are shown in Figure 3 and SFigure 3 in the SI. At 300 K, the $\chi_{\text{M}}T$ value of **1**, $1.2 \text{ cm}^3 \text{ K mol}^{-1}$, denotes a relevant amount of the Fe^{II} centers in the LS state, in agreement with the ^{57}Fe Mössbauer spectra recorded at 295 K (Figure 2). The

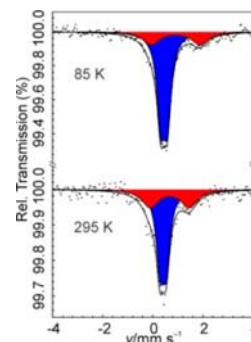


Figure 2. Mössbauer spectra of **1** measured at 85 and 295 K.

Mössbauer spectra consist of two doublets. The characteristic isomer shift (δ , relative to α -iron) and quadrupole splitting (ΔE_{Q}) parameters are 0.680(91) and $1.56(19) \text{ mm s}^{-1}$ for the HS doublet and 0.413(16) and $0.244(31) \text{ mm s}^{-1}$ for the LS doublet. The populations in the HS and LS states deduced from the least-squares fit routine analysis of the spectra are 35 and 65%, respectively. Upon lowering of the temperature to 85 K, the population of the LS doublet increases by 10% at the expense of the HS doublet. The parameters δ and ΔE_{Q} practically remain constant for the LS doublet, while they increase for the HS doublet (STable 3 in the SI).

Upon warming from 300 to 400 K, the $\chi_{\text{M}}T$ value for **1** experiences an abrupt increase up to $3.65 \text{ cm}^3 \text{ K mol}^{-1}$, a value that falls into the range of values expected for 100% of the Fe^{II} centers in the HS state. This change in the magnetic susceptibility is not due to a thermal SCO of **1**. Dehydration of **1** and concomitant transformation into **2** take place in this temperature interval.

Figure 3 illustrates the $\chi_{\text{M}}T$ versus T curve for **2** in the cooling and warming modes. Compound **2** undergoes a continuous and incomplete thermal SCO behavior in the temperature interval of 300–100 K. Below this temperature, $\chi_{\text{M}}T$ drops to $1.0 \text{ cm}^3 \text{ K mol}^{-1}$ at 5 K because of the zero-field splitting (ZFS) of the Fe^{II} centers that remain in the HS state. The palladium analogues, compounds **3** and **4**, exhibit magnetic behavior identical with described for **1** and **2**, respectively.

In contrast to **1** and **2**, the hydrated nickel derivative, compound **5**, presents at 300 K a $\chi_{\text{M}}T$ value of $3.0 \text{ cm}^3 \text{ K mol}^{-1}$. The magnetic susceptibility decreases progressively to $1.5 \text{ cm}^3 \text{ K mol}^{-1}$ (100 K) because of the thermal SCO of approximately 50% of the Fe^{II} centers. A further lowering of $\chi_{\text{M}}T$ is ascribed to the ZFS of the paramagnetic Fe^{II} ions. Compound **6** behaves similarly to **5**, but the temperature at which the thermal SCO takes place is shifted 50 K downward.

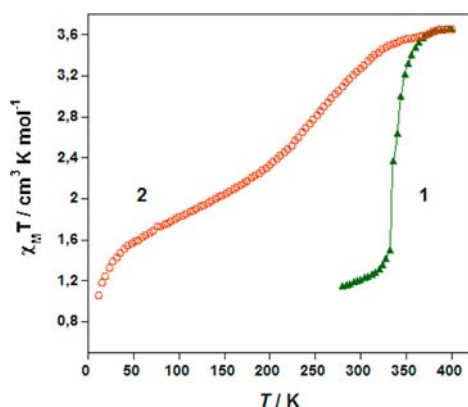


Figure 3. Magnetic properties of **1** and **2** in the form of $\chi_M T$ versus T .

In these coordination polymers, the hydration–dehydration process is totally reversible and the ST properties are recovered at will. The hydrated compounds are dark yellow, while the dehydrated ones are light yellow. In general, the inclusion of H_2O molecules in the framework leads to stabilization of the Fe^{II} ions in the LS state. It is well-known that solvent molecules may provoke dramatic changes in the ST behavior via subtle electronic effects and/or structural modifications. In this respect, similar drastic changes have already been observed for the azpy, dpe, and bpac homologues.^{11–15} However, in general, it is difficult to explain the role of the solvent molecule in terms of host–guest interactions and more particularly in the title compounds because the invited H_2O molecules in **1** are strongly disordered.

To find the experimental synthetic conditions to avoid chloratration of the pillar ligand in favor of the inclusion of different functional guest molecules is ongoing work in our laboratory.

■ ASSOCIATED CONTENT

📄 Supporting Information

X-ray crystallographic data in CIF format, experimental details, synthetic pathways, additional crystal data, TGA, PXRD, magnetic and Mössbauer properties, and IR spectra. This material is available free of charge via the Internet at <http://pubs.acs.org>.

■ AUTHOR INFORMATION

✉ Corresponding Author

*E-mail: jose.a.real@uv.es.

Notes

The authors declare no competing financial interest.

■ ACKNOWLEDGMENTS

This work was supported by the Spanish Ministerio de Ciencia e Innovación (MICINN) and FEDER funds (CTQ2010-18414) and the Generalitat Valenciana (ACOMP2012/233 and PROMETEO2012/049). We acknowledge Prof. P. Gütllich for helpful discussions and for providing Mössbauer spectroscopy facilities. F.J.M.-L. thanks the MICINN for a predoctoral (FPI) fellowship.

■ REFERENCES

(1) (a) Kitagawa, S.; Kitaura, R.; Noro, S. *Angew. Chem., Int. Ed.* **2004**, *43*, 2334. (b) Kitagawa, S.; Matsuda, R. *Coord. Chem. Rev.* **2007**,

251, 2490. (c) Férey, G. *Chem. Soc. Rev.* **2008**, *37*, 191. (d) Corma, A.; García, H.; Llabres, I.; Xamena, F. X. *Chem. Rev.* **2010**, *110*, 4606.

(2) Dechambenoit, P.; Long, J. R. *Chem. Soc. Rev.* **2011**, *40*, 3249.

(3) (a) Rocha, J.; Carlos, L. D.; Almeida Paz, F. A.; Ananias, D. *Chem. Soc. Rev.* **2011**, *40*, 926. (b) Liu, D.; Huxford, R. C.; Lin, W. *Angew. Chem., Int. Ed.* **2011**, *50*, 3696.

(4) (a) Avendano, C.; Zhang, Z.; Ota, A.; Zhao, H.; Dunbar, K. R. *Angew. Chem., Int. Ed.* **2011**, *50*, 6543. (b) Shimomura, S.; Kitagawa, S. *J. Mater. Chem.* **2011**, *21*, 5537.

(5) (a) Shigematsu, A.; Yamada, T. H.; Kitagawa, H. *J. Am. Chem. Soc.* **2011**, *133*, 2034. (b) Bureekaew, S.; Higuchi, S. T.; Kawamura, T.; Tanaka, D.; Yanai, N.; Kitagawa, S. *Nat. Mater.* **2009**, *8*, 831.

(6) (a) Gütllich, P.; Goodwin, H. A., Eds. *Spin Crossover in Transition Metal Compounds. Topics in Current Chemistry*; Springer: New York, 2004; pp 233–235. (b) Real, J. A.; Gaspar, A. B.; Muñoz, M. C. *Dalton Trans.* **2005**, 2062. (c) Gaspar, A. B.; Ksenofontov, V.; Seredyuk, M.; Gütllich, P. *Coord. Chem. Rev.* **2005**, *249*, 2661. (d) Real, J. A.; Muñoz, M. C. *Coord. Chem. Rev.* **2011**, *255*, 2068. (e) Bousseksou, A.; Molnár, G.; Demont, P.; Menegotto, J. *Mater. Chem.* **2003**, *13*, 2069.

(7) (a) Kahn, O.; Martinez, C. J. *Science* **1998**, *279*, 44. (b) Galet, A.; Gaspar, A. B.; Muñoz, M. C.; Bukin, G. V.; Levchenko, G.; Real, J. A. *Adv. Mater.* **2005**, *17*, 2949. (c) Bousseksou, A.; Molnár, G.; Salmon, L.; Nicolazzi, W. *Chem. Soc. Rev.* **2011**, *40*, 3313.

(8) Real, J. A.; Andrés, E.; Muñoz, M. C.; Julve, M.; Granier, T.; Bousseksou, A.; Varret, F. *Science* **1995**, *268*, 265.

(9) (a) Halder, G. J.; Kepert, C. J.; Moubaraki, B.; Murray, K. S.; Cashion, J. D. *Science* **2002**, *298*, 1762. (b) Neville, S. M.; Halder, G. J.; Chapman, K. W.; Duriska, M. B.; Southon, P. D.; Cashion, J. D.; Létard, J. F.; Moubaraki, B.; Murray, K. S.; Kepert, C. J. *J. Am. Chem. Soc.* **2008**, *130*, 2869.

(10) (a) Niel, V.; Martinez-Agudo, J. M.; Muñoz, M. C.; Gaspar, A. B.; Real, J. A. *Inorg. Chem.* **2001**, *40*, 3838. (b) Ohba, M.; Yoneda, K.; Agustí, G.; Muñoz, M. C.; Gaspar, A. B.; Real, J. A.; Yamasaki, M.; Ando, H.; Nakao, Y.; Sakaki, S.; Kitagawa, S. *Angew. Chem., Int. Ed.* **2009**, *48*, 4767. (c) Southon, P. D.; Liu, L.; Fellows, E. A.; Price, D. J.; Halder, G. J.; Chapman, K. W.; Moubaraki, B.; Murray, K. S.; Létard, J. F.; Kepert, C. J. *J. Am. Chem. Soc.* **2009**, *131*, 10998.

(11) Agustí, G.; Ohtani, R.; Yoneda, K.; Gaspar, A. B.; Ohba, M.; Sánchez-Royo, J. F.; Muñoz, M. C.; Kitagawa, S.; Real, J. A. *Angew. Chem., Int. Ed.* **2009**, *48*, 8944.

(12) Ohtani, R.; Yoneda, K.; Furukawa, S.; Horike, N.; Kitagawa, S.; Gaspar, A. B.; Muñoz, M. C.; Real, J. A.; Ohba, M. *J. Am. Chem. Soc.* **2011**, *133*, 8600.

(13) Agustí, G.; Cobo, S.; Gaspar, A. B.; Molnár, G.; Ould Moussa, N.; Szilágyi, P. A.; Pálfi, V.; Vieu, C.; Muñoz, M. C.; Real, J. A.; Bousseksou, A. *Chem. Mater.* **2008**, *20*, 6721.

(14) Bartual-Murgui, C.; Ortega-Villar, N. A.; Shepherd, H. J.; Muñoz, M. C.; Molnár, G.; Salmon, L.; Bousseksou, A.; Real, J. A. *J. Mater. Chem.* **2011**, *21*, 7217.

(15) Muñoz Lara, F. J.; Gaspar, A. B.; Muñoz, M. C.; Arai, M.; Kitagawa, S.; Ohba, M.; Real, J. A. *Chem.—Eur. J.* **2012**, *18*, 8013.

(16) Champness, N. R.; Khlobystov, A. N.; Majuga, A. G.; Schröder, M.; Zyk, N. V. *Tetrahedron Lett.* **1999**, *40*, 5413.